Autonomous Fire Monitor System – Initial Studies

Mateusz Pluskota, Krzysztof Schwierz
KBA AUTOMATIC Sp. z o.o., Technologiczna street 2A, 45-839 Opole

Andrzej Neumann, Dominik Fila, Łukasz Paczkowski, Paweł Majewski
Opole University of Technology, Faculty of Electrical Engineering, Automatic Control and Informatics, Prószkowska street 76, 45-758 Opole

Abstract: In this paper, preliminary studies dedicated to facilitating the development of a control algorithm for an autonomous fire monitor have been presented. Using the Lagrange method, a dynamic model of the system has been determined, and two control algorithms have been verified. The applied adaptive algorithm yielded satisfactory regulation results, even when object parameters differed from the model by 10%. The manuscript also presents the hardware layer of the developed prototype, which consists of a fire monitor, a control system based on a programmable logic controller, and a vision system that enables the automatic localization of high temperature points in a 3D space.

Keywords: fire monitor, dynamic equations, adaptive control, inverse kinematics

1. Introduction

Fires in modern automation are among the most hazardous phenomena, posing a significant threat to human life and infrastructure. In industrial settings, the risk of starting a fire is particularly high, often resulting from flammable materials, high temperatures, or open flames as part of technological processes [1–3]. For this reason, the field of firefighting is rapidly evolving, seeking the fastest and most effective methods for eliminating fires [4–7].

Commonly used sprinklers are far from a perfect solution. Simply triggering the extinguishing action of such a system requires hot air, which is caused by an already growing fire. Depending on the conditions and the height of the sprinkler system, activation can occur anywhere from several seconds to several minutes, allowing the fire to amplify and spread. Furthermore, the sprinkler system covers the entire area, not just the fire. Therefore, autonomous fire extinguishing towers equipped with fire detection sensors are increasingly used, which operate faster and specifically eliminate the fire in its infancy [8, 9].

The range of possibilities for connecting fire detection systems to the extinguishing tower is wide. Fire detection systems typically incorporate some form of camera system. Cameras can analyze images for color and brightness; the combination of these factors indicates the detection of a flame. Similarly, YOLO (You Only Look Once) neural networks can detect and localize fire [10–12]. However, this solution is associated with inaccuracy; sunlight reflecting off a shiny object may be interpreted as flame, while, for example, hot coals may not be recognized as a threat. A solution to this problem is the use of infrared cameras, which can detect high temperatures. Reflected light does not affect this measurement, and a smoldering fire can be detected. Using two cameras allows for the localization of a fire in three-dimensional space, thanks to stereovision [13–15].

In this paper, we introduce initial studies concerning the novel automatic control of a fire monitor. Thanks to the special connection of actuators, PLC (Programmable Logic Controller), and system vision, it was possible to develop the autonomous fire extinguishing system. Therefore, the novelty of the paper can be summarized as follows:

- Determine the dynamic equations of the fire monitor by using the Lagrange method.
- Implementation and verification of inverse dynamics control and modified MRAC (Model Reference Adaptive Control) in MATLAB/Simulink.
- Introduce the physical prototype of the fire monitor system based on LiDAR (Light Detection and Ranging) and thermal imaging camera.

The manuscript is organized as follows. After the Introduction, the dynamic equations of the fire monitor model are presented in Section 2. Consequently, the Simulation studies concerning the two control approaches are given in Section 3. A hardware prototype is presented in the following paragraph, immediately preceding the Conclusions and Open Problems section, which, together with the Appendix, concludes the paper.

2. Dynamic equations

The dynamic model of the system described by the scheme in Fig. 1 has been determined using the Lagrange method.

The mentioned plant has only two rotating degrees of freedom. First, in the horizontal plane, and second, perpendicular to the base plane, respectively. Mentioned joins are depicted in Fig. 1 in red color, and in mathematical considerations, both have been assumed as generalized variables; therefore, the appropriate equations have the following form

Autor korespondujący:
Paweł Majewski, p.majewski@po.edu.pl

Artykuł recenzowany
nadesłany 16.12.2025 r., przyjęty do druku 14.05.2026 r.

Symbols

$\mathbf{e}(t)$ – error signal vector
J_{ISE} – performance index ISE
J_{ITAE} – performance index ITAE
J_{ITSE} – performance index ITSE
$J_1,\ J_2,\ J_2'$ – moments of inertia
$K_r,\ K_x$ – MRAC gains
L – Lagrangian function
l_0 – height of the robot
$l_{m1},\ l_{m2}$ – respective centers of mass distances
$M_{q1},\ M_{q2}$ – driving torques
$m_1,\ m_2$ – masses of appropriate members
$\mathbf{q}(\mathrm{t})$ – vector of generalized variables
$\mathbf{q}_{\mathrm{d}}(\mathrm{t})$ – desired vector of generalized variables
$q_1(t),\ q_2(t)$ – joint rotation angles-generalized variables
T – kinetic energy
U – potential energy
$x_{1,2},\ y_{1,2},\ z_{1,2}$ – primary variables
$\mathbf{y}_{\mathrm{ref}}(t)$ – reference value/setpoint
$\alpha_{1,2}$ – correction factor
$(\dot{\cdot}),\ (\ddot{\cdot})$ – first- and second-degree time derivative

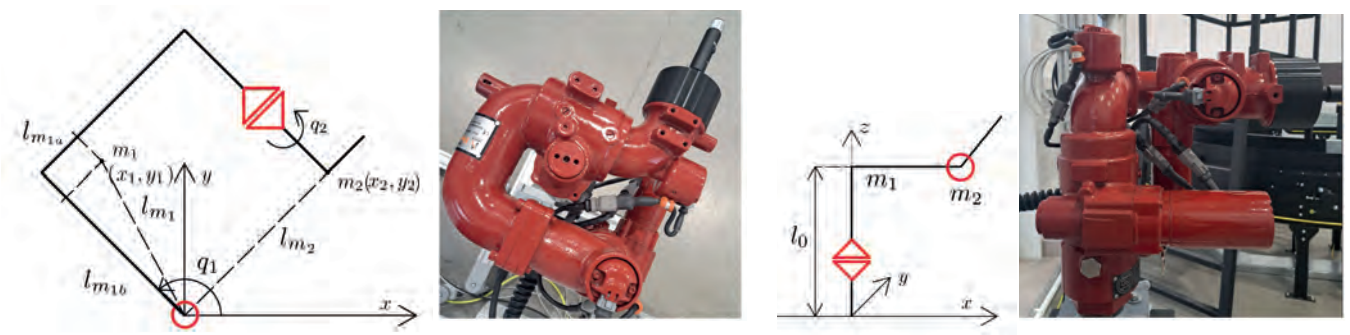

a) Top view of the system

(b) Side view of the system

Fig. 1. Schematic diagram of the fire monitor system with a real view
Rys. 1. Schemat działka gaśniczego wraz z widokiem rzeczywistym

$$\frac{d}{dt}\left(\frac{\partial L}{\partial \dot{q}_1}\right)+\frac{\partial L}{\partial \dot{q}_1}=M_{q_1},$$

$$\frac{d}{dt}\left(\frac{\partial L}{\partial \dot{q}_2}\right)+\frac{\partial L}{\partial \dot{q}_2}=M_{q_2}, \tag{1}$$

where

$$L\left(\mathbf{q}(t),\dot{\mathbf{q}}(t),t\right)=T\left(\mathbf{q}(t),\dot{\mathbf{q}}(t),t\right)-U\left(\mathbf{q}(t),\dot{\mathbf{q}}(t),t\right), \tag{2}$$

is an energy potential (Lagrangian). The particular members of Eqn. (2), are kinetic and potential energies which are given as follows

$$T=\frac{1}{2}m_1\left(\dot{x}_1^2+\dot{y}_1^2+\dot{z}_1^2\right)+\frac{1}{2}J_1\dot{q}_1^2+$$
$$+\frac{1}{2}m_2\left(\dot{x}_2^2+\dot{y}_2^2+\dot{z}_2^2\right)+\frac{1}{2}J_2\dot{q}_1^2+\frac{1}{2}J_2'\dot{q}_2^2, \tag{3}$$

and

$$U=m_1gz_1+m_2gz_2, \tag{4}$$

where $z_1=z_2=l_0$ (see Fig. 1(b)). The Eqns. (3) and (4) are determined using primary variables. Therefore, the relationship between generalized ones, based on Fig. (1(a)), can be written as

$$x_1=l_{m_1}\cos\left(q_1-\arccos\left(\frac{l_{m_{1b}}}{l_{m_1}}\right)\right),$$
$$y_1=l_{m_1}\sin\left(q_1-\arcsin\left(\frac{l_{m_{1a}}}{l_{m_1}}\right)\right),$$
$$z_1=l_0,$$
$$x_2=l_{m_2}\cos\left(q_1-\frac{\pi}{2}\right), \tag{5}$$
$$y_2=l_{m_2}\sin\left(q_1-\frac{\pi}{2}\right),$$
$$z_2=l_0,$$

and

$$\dot{x}_1=-l_{m_1}\dot{q}_1\sin\left(q_1-\arccos\left(\frac{l_{m_{1b}}}{l_{m_1}}\right)\right),$$
$$\dot{y}_1=l_{m_1}\dot{q}_1\cos\left(q_1-\arcsin\left(\frac{l_{m_{1a}}}{l_{m_1}}\right)\right),$$
$$\dot{z}_1=0,$$
$$\dot{x}_2=-l_{m_2}\dot{q}_1\sin\left(q_1-\frac{\pi}{2}\right), \tag{6}$$
$$\dot{y}_2=l_{m_2}\dot{q}_1\cos\left(q_1-\frac{\pi}{2}\right),$$
$$\dot{z}_2=0.$$

Due to the following dependency

$$\arccos\left(\frac{l_{m_{1b}}}{l_{m_1}}\right) = \arcsin\left(\frac{l_{m_{1a}}}{l_{m_1}}\right), \tag{7}$$

the obtained Lagrangian is given as follows

$$\begin{aligned} L = T - U &= \frac{1}{2}m_1\left\{l_{m_1}^2\dot{q}_1^2\sin^2\left(q_1 - \arccos\left(\frac{l_{m_{1b}}}{l_{m_1}}\right)\right)\right. + \\ &\left. + l_{m_1}^2\dot{q}_1^2\cos^2\left(q_1 - \arccos\left(\frac{l_{m_{1b}}}{l_{m_1}}\right)\right)\right\} + \frac{1}{2}J_1\dot{q}_1^2 \\ &+ \frac{1}{2}m_2\left\{l_{m_2}^2\dot{q}_1^2\sin^2\left(q_1 - \frac{\pi}{2}\right) + l_{m_2}^2\dot{q}_1^2\cos^2\left(q_1 - \frac{\pi}{2}\right)\right\} + \\ &+ \frac{1}{2}J_2\dot{q}_1^2 + \frac{1}{2}J_2'\dot{q}_2^2 - m_1gz_1 - m_2gz_2 \\ &= \frac{1}{2}m_1l_{m_1}^2\dot{q}_1^2 + \frac{1}{2}m_2l_{m_2}^2\dot{q}_1^2 + \frac{1}{2}J_1\dot{q}_1^2 + \frac{1}{2}J_2\dot{q}_1^2 + \\ &+ \frac{1}{2}J_2'\dot{q}_2^2 - m_1gz_1 - m_2gz_2, \end{aligned} \tag{8}$$

after taking into account Eqn. (1) we finally end with the following dynamic equations

$$\begin{cases} m_1l_{m_1}^2\ddot{q}_1 + m_2l_{m_2}^2\ddot{q}_1 + J_1\ddot{q}_1 + J_2\ddot{q}_1 = M_{q_1}, \\ J_2'\ddot{q}_2 = M_{q_2}. \end{cases} \tag{9}$$

Having the necessary formulas, we can proceed to the implementation in a simulation environment in the next section.

3. Simulation studies

To validate the control capabilities of a fire monitor (Eqn. (9)), a comprehensive system using the parameters described in Table 1 has been developed and implemented in the MATLAB/Simulink environment (including DSP toolbox). The developed virtual control system environment, next to the dynamic model, incorporates elements related to inverse kinematics, motion trajectory, and control systems based on inverse dynamics and the MRAC approach. For clarity, a description of the most relevant composed modules is provided in the appendix section 6. The assumed performance index for comparative analysis, in addition to time-domain graphs, is the Integral of Squared Error (ISE)

$$J_{\text{ISE}} = \int_0^{t_s} e^2(t)dt, \tag{10}$$

Integral of Time-Weighted Absolute Error (ITAE)

$$J_{\text{ITAE}} = \int_0^{t_s} t\left|e(t)\right|dt, \tag{11}$$

Table 1. The simulation parameters
Tabela 1. Parametry symulacji

Parameter	Value	Unit
J_1	0.074 + 0.111	[kg · m²]
J_2	0.001 + 0.043	[kg · m²]
J_2'	0.002 + 0.19	[kg · m²]
l_{m_1}	0.234	[m]
l_{m_2}	0.37	[m]
m_1	10.4	[kg]
m_2	0.6 + 0.2	[kg]

and Integral of Time-Weighted Squared Error (ITSE)

$$J_{\text{ITSE}} = \int_0^{t_s} te^2(t)dt, \tag{12}$$

where each simulation instance was performed with a fixed step size and time duration.

This section presents the results of simulation studies for two separate approaches; therefore, the control strategies used are discussed in the following subsections.

3.1. The Inverse dynamics control

The Inverse dynamics control approach employed in the first simulation studies relies on tracking the motion trajectory generated by inverse kinematics. Based on the Cartesian coordinates of the hot spot determined by the vision system and the monitor's targeting point, internal variable values are calculated and fed into the inverse object model. This approach generates control signals that, when input to the model, produce the expected accelerations. In the ideal case, the inverse model resulted in precise control Figs. 2 and 3.

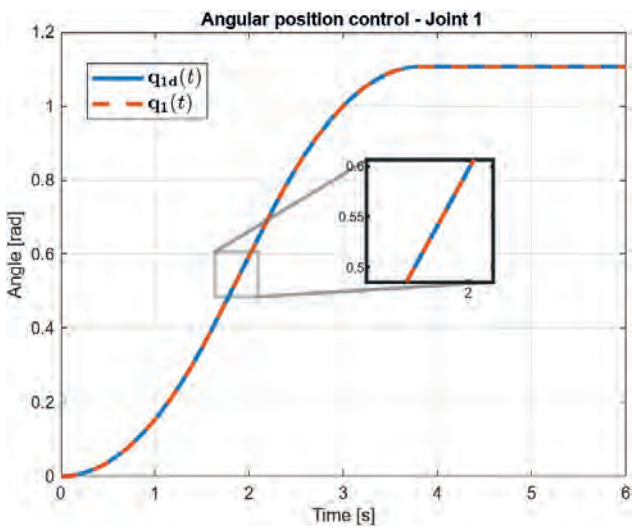

Fig. 2. Inverse dynamics control result of joint 1 – basic model, $J_{\text{ISE}} = 1.78 \cdot 10^{-5}$
Rys. 2. Wynik sterowania metodą dynamiki odwrotnej złącza 1 – model podstawowy, $J_{\text{ISE}} = 1{\cdot}78 \cdot 10^{-5}$

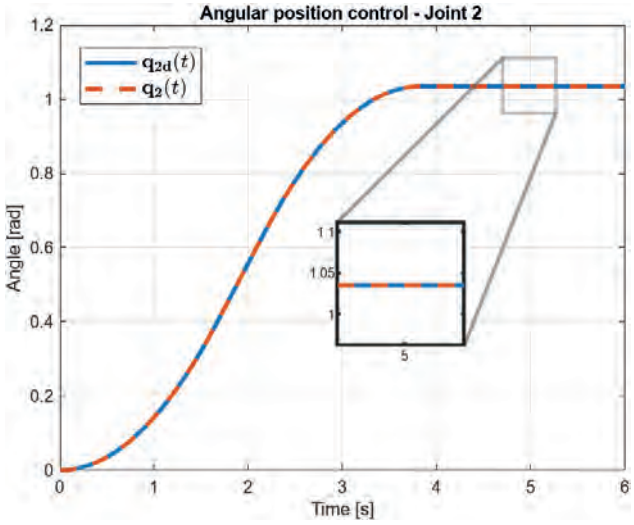

Fig. 3. Inverse dynamics control result of joint 2 – basic model, $J_{ISE} = 1.372 \cdot 10^{-5}$
Rys. 3. Wynik sterowania metodą dynamiki odwrotnej złącza 2 – model podstawowy, $J_{ISE} = 1.372 \cdot 10^{-5}$

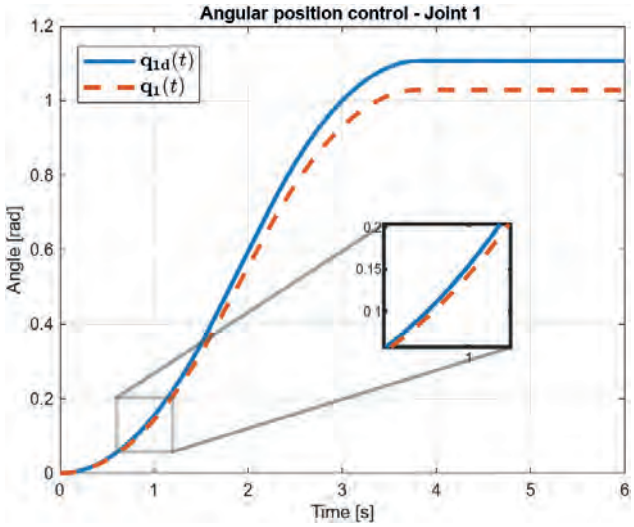

Fig. 4. Inverse dynamics control result of joint 1 – model with 10% weight difference, $J_{ISE} = 21.91, J_{ITAE} = 1.231, J_{ITSE} = 0.091$
Rys. 4. Wynik sterowania metodą dynamiki odwrotnej złącza 1 – model z 10 % różnicą mas, $J_{ISE} = 21.91, J_{ITAE} = 1.231, J_{ITSE} = 0.091$

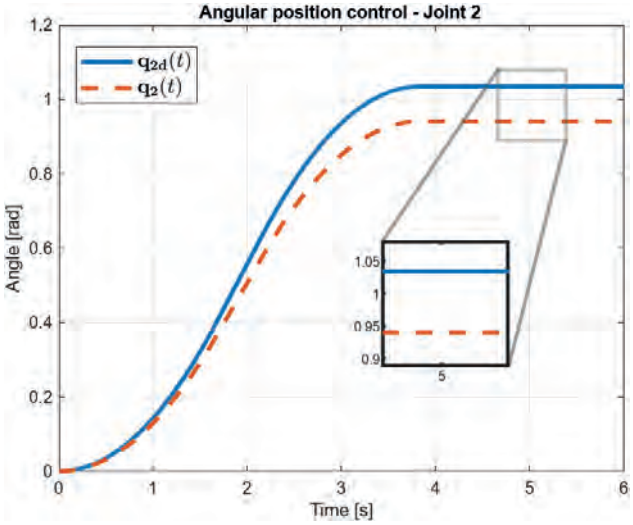

Fig. 5. Inverse dynamics control result of joint 2 – model with 10% weight difference, $J_{ISE} = 32.16, J_{ITAE} = 1.491, J_{ITSE} = 0.133$
Rys. 5. Wynik sterowania metodą dynamiki odwrotnej złącza 2 – model z 10 % różnicą mas, $J_{ISE} = 32.16, J_{ITAE} = 1.491, J_{ITSE} = 0.133$

Unfortunately, the described approach has a significant disadvantage in cases where the differences resulting from the inverted model and the real object exceed 10% of the mass of individual elements; this control is no longer acceptable (Figs. 4 and 5). The assumed expected difference in the masses of the particular robot sections results from considering the medium factor flowing through its interior.

To achieve greater accuracy, adaptive control is employed in the following subsection.

3.2. The MRAC control method

Regarding various control strategies in the literature, the commonly used solutions include, e.g., PID or SMC (Sliding Mode Control). In our approach, to improve the control process of the simulation fire monitor model, a regulation method based on MRAC was proposed (Fig. 6). The mentioned approach is

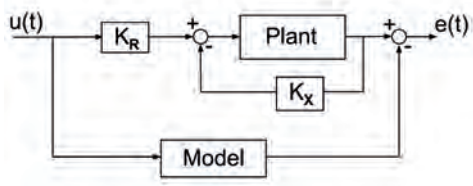

Fig. 6. The MRAC controller
Rys. 6. Regulator typu MRAC

an adaptive control algorithm in which the coefficients of the appropriate gains are determined based on the MIT rule that minimizes the performance index [16]

$$Pi = \frac{1}{2}\mathbf{e}(t)^2, \tag{13}$$

where $\mathbf{e}(t)\mathbf{q}_{\text{plant}}(t) - \mathbf{q}_{\text{model}}(t)$. For more details see Ref. [16]

and Appendix section. The MRAC algorithm works correctly even with large differences between the object and the model. Here, as in the second case in the Inverse Dynamic Control section, the mass of the plant members was 10% greater than in the model.

In our approach, the mentioned MRAC method was not fully utilized, as minor changes were introduced to the algorithm for determining changes in the correction coefficients K_r and K_x (Fig. 6). These parameters can be determined using the formula [16]

$$\begin{aligned} \frac{d}{dt}K_r &= -\alpha_1 e \frac{\partial e(t)}{\partial K_r}, \\ \frac{d}{dt}K_x &= -\alpha_2 e \frac{\partial e(t)}{\partial K_x}. \end{aligned} \tag{14}$$

In our research, a slight simplification was adopted:

$$\begin{aligned} \frac{\partial e}{\partial K_r} &\approx \frac{\Delta e}{\Delta K_r}, \\ \frac{\partial e}{\partial K_x} &\approx \frac{\Delta e}{\Delta K_x}. \end{aligned} \tag{15}$$

Nevertheless, the accepted assumptions proved to be surprisingly effective, as confirmed by the control process results in Figures 7–10 and the performance indexes.

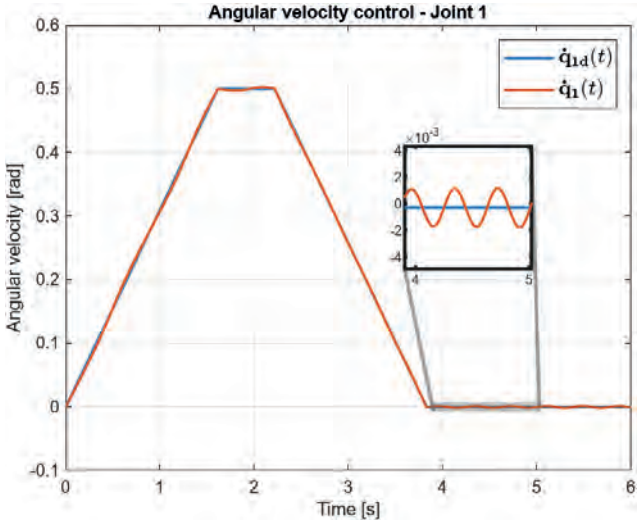

Fig. 7. The MRAC control result of joint 1 – angular velocity
Rys. 7. Wynik sterowania metodą MRAC złącza 1 – prędkość kątowa

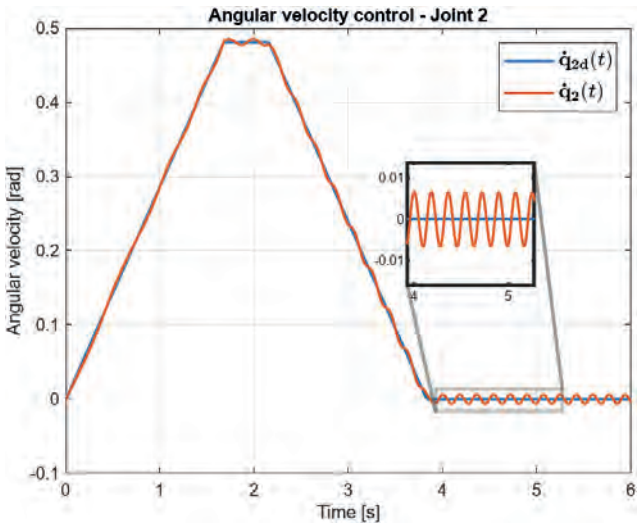

Fig. 8. The MRAC control result of joint 2 – angular velocity
Rys. 8. Wynik sterowania metodą MRAC złącza 2 – prędkość kątowa

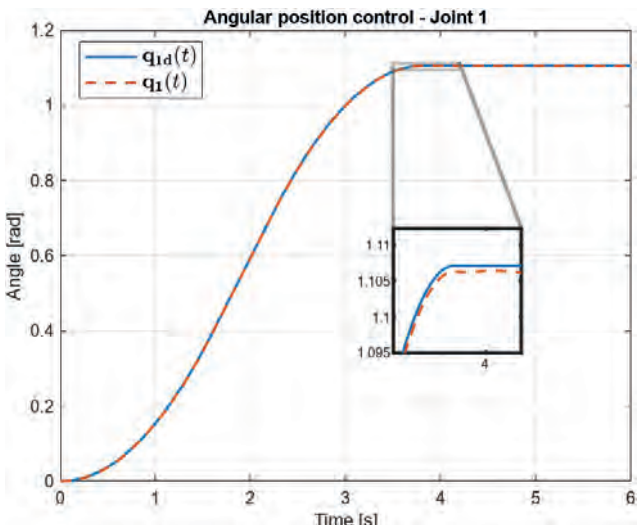

Fig. 9. The MRAC control result of joint 1 – angular position, $J_{ISE} = 2.086 \cdot 10^{-4}$, $J_{ITAE} = 1.411 \cdot 10^{-2}$, $J_{ITSE} = 2.23 \cdot 10^{-5}$
Rys. 9. Wynik sterowania metodą MRAC złącza 1 – położenie kątowe, $J_{ISE} = 2.086 \cdot 10^{-4}$, $J_{ITAE} = 1.411 \cdot 10^{-2}$, $J_{ITSE} = 2.23 \cdot 10^{-5}$

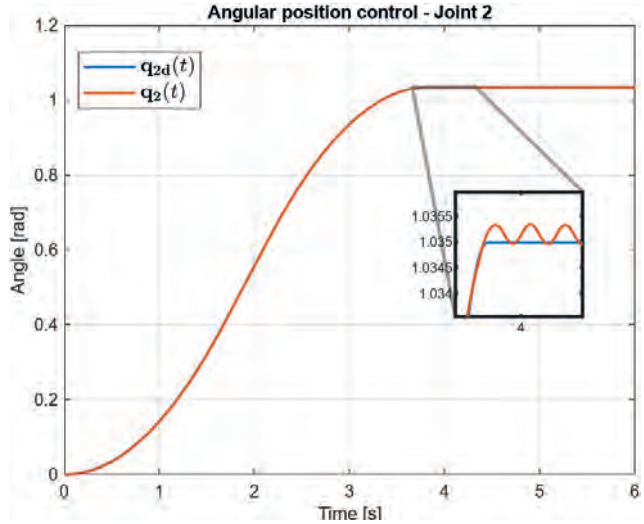

Fig. 10. The MRAC control result of joint 2 – angular position, $J_{ISE} = 2.911 \cdot 10^{-4}$, $J_{ITAE} = 1.207 \cdot 10^{-2}$, $J_{ITSE} = 1.648 \cdot 10^{-5}$
Rys. 10. Wynik sterowania metodą MRAC złącza 2 – położenie kątowe, $J_{ISE} = 2.911 \cdot 10^{-4}$, $J_{ITAE} = 1.207 \cdot 10^{-2}$, $J_{ITSE} = 1.648 \cdot 10^{-5}$

Having considered the necessary theoretical aspects, let us now turn to the physical realization.

4. Hardware realization

The KBA AUTOMATIC company developed the Autonomous Fire Monitor System based on the real-life objects described in Table 2.

Table 2. A list of the most important system components
Tabela 2. Zestawienie najważniejszych elementów systemu

No.	Module	Model
1	Fire monitor	STYLE 3463 FIREFOX
2	Programmable Logic Controller	S7-1518TF
3	Thermal imaging camera	Flir A70
4	Lens	FOV 95o
5	LiDAR	Ouster OS1

Fig. 11. The real-life fire monitor
Rys. 11. Rzeczywisty obiekt działka gaśniczego

Fig. 12. Thermal imaging camera (left) and LiDAR system (right)
Rys. 12. Kamera termowizyjna (po lewej) oraz system LiDAR (po prawej)

Fig. 13. Developed control cabinet
Rys. 13. Opracowana szafa sterownicza

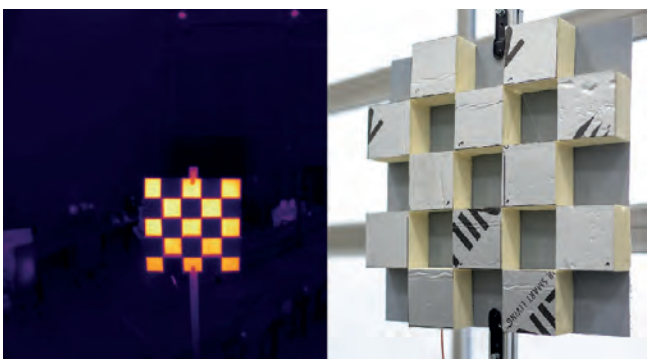

Fig. 14. Hot spot mockup prepared for verification tests – thermal imaging (left) and real-life (right) view
Rys. 14. Makieta gorącego punktu przygotowana do testów weryfikacyjnych – obraz termiczny (po lewej) i widok rzeczywisty (po prawej)

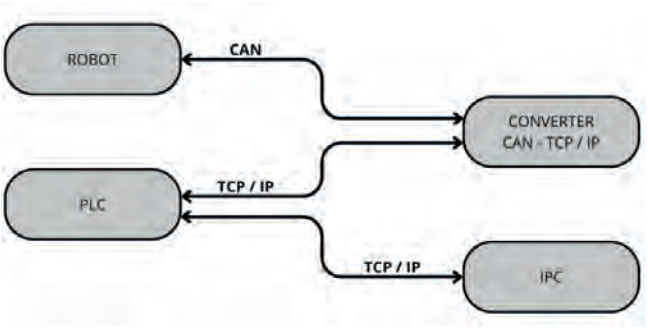

Fig. 15. The connection diagram of the fire monitor system objects
Rys. 15. Schemat połączeń obiektów systemu działka gaśniczego

The entire prototype consists of two components: a fire extinguishing module (Fig. 11) and a hot spot detection and localization module (Fig. 12), which are managed from the hardware implemented in the control cabinet (Fig. 13).

The detection and localization structure is based on software running on an industrial computer, which works in conjunction with a thermal imaging camera to detect hot spots and one/two LiDAR sensors positioned at different locations. This solution allows for the precise location of the point requiring cooling (Fig. 14) without using any AI (Artificial Intelligence). Once the hot spot coordinates are determined, the data is transmitted via TCP/IP to the PLC. The controller calculates inverse kinematics and sends joint variables via TCP/IP communication, which are then converted by a converter to CAN communication that controls the robotic arm. The mentioned communication path is described in Fig. 15.

The fire monitor itself operates at a working pressure of approximately 10 bar, which allows for a practically straight-line water jet at a distance of up to 20 m from the developed system. A higher-capacity pump is planned, allowing for a future increase in this range to 30 m. Therefore, a straight-line water jet trajectory was assumed in our work, omitting the calculation of the ballistic curve. Consequently, after aiming, the water jet should effectively cool the detected hot spot, and if necessary, the monitor can automatically direct the nozzle to the next area requiring cooling.

As part of preliminary testing to verify the effectiveness of the real-life system, a laser pointer was placed on the end effector. This approach allowed us to confirm the prototype's correct operation by aiming the laser beam at the detected hot spot.

5. Conclusions and open problems

In this paper, an initial study on the control of the Autonomous Fire Monitor System has been presented. We have introduced the dynamic model of the system, derived from

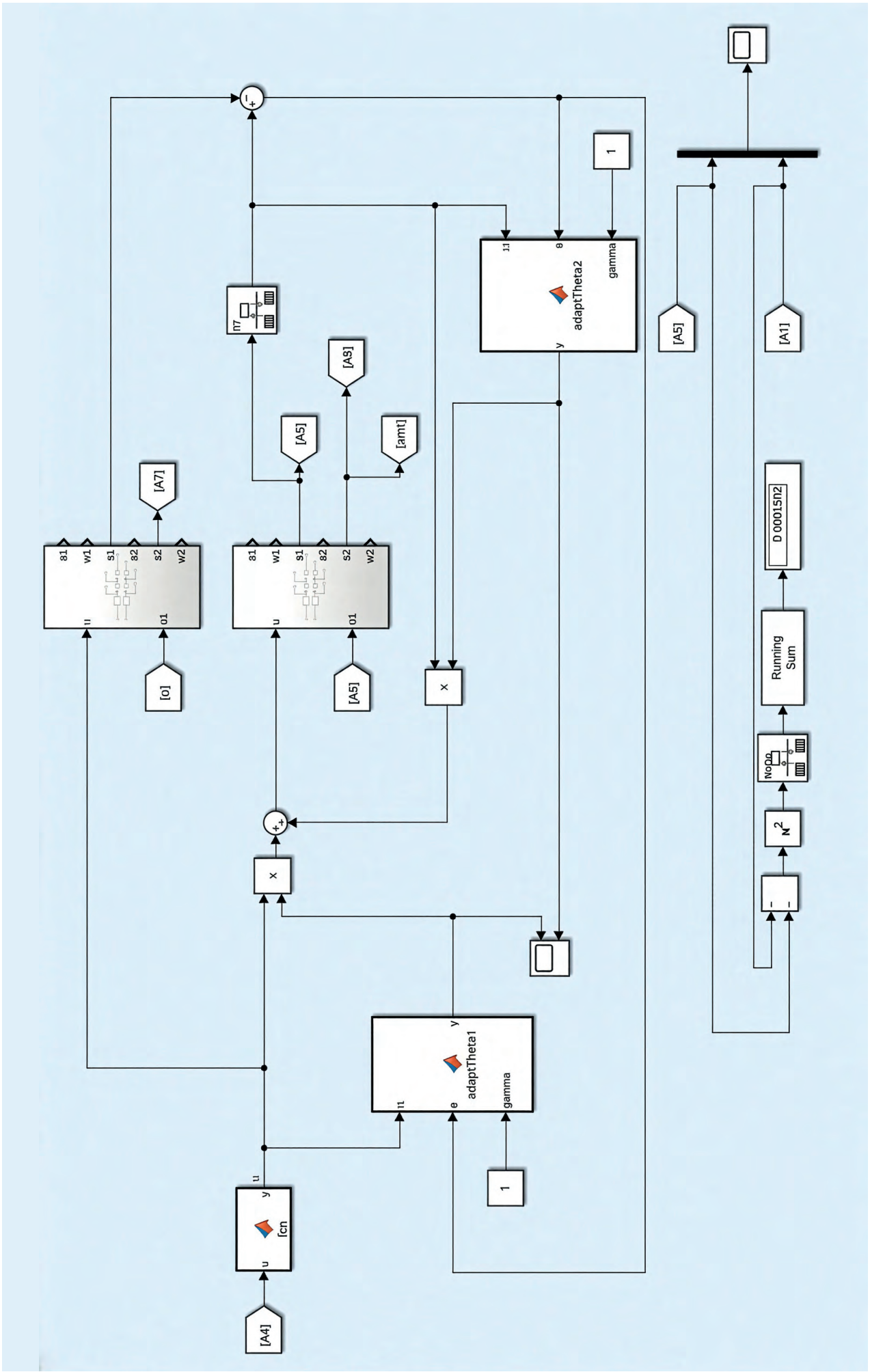

Fig. 16. Implementation of the MRAC method in MATLAB/Simulink
Rys. 16. Implementacja metody MRAC w środowisku MATLAB/Simulink

the Lagrange method, and described simulation studies performed in the MATLAB/Simulink environment. Our plant, the so-called digital twin object, has been controlled using Inverse Model Control and a slightly modified Model Reference Adaptive Controller. In addition to the theoretical results, a physical realization on a real-life system has been proposed. According to the designed compatibility between the motion system, vision system, and control layer, we have developed a beneficial Autonomous Fire Monitor System that can be utilized in various industrial automation tasks.

6. Appendix

This paragraph presents the modules of the developed system used in the Simulation studies section of this paper. The primary component of the plant is the dynamic model, which incorporates inverse kinematics, inverse model control, and MRAC methodology.

At the beginning, the trajectory generation process is initiated. After entering the global coordinates (*x, y, z*) of the beginning and end position of the end-effector, the joint variable vectors are determined using Inverse Kinematics. Because the analyzed object is essentially a two-degree-of-freedom manipulator with revolute joints, the inverse kinematics equations require trigonometric functions. In the next step, after specifying the robot's motion execution time, the velocities and accelerations are calculated based on the system's trapezoidal motion profile. Worth mentioning in the described step, the maximum velocities and accelerations are determined by the motors' motion parameters. The result of the detailed stage is a vector of desired variables $\mathbf{q}_{\mathrm{d}}(t) = \left(\mathbf{q}(t), \dot{\mathbf{q}}(t), \ddot{\mathbf{q}}(t)\right)$ with a trapezoidal motion profile.

The received reference values feed two modules, the Inverse Dynamics Control and the MRAC control. In the first scenario, based on the $\mathbf{q}_{\mathrm{d}}(t)$, the required system driving torques are determined, which constitute input signals to the Forward Dynamics defined by Eqn. (9). Simulation studies from this type of control can be found in part 3.1 of Section 3.

The last element of the developed virtual system is the MRAC control depicted in Fig. 16. The mentioned algorithm aims to control the object output in accordance with the designed model, even in the absence of time-invariant properties or a mismatch between the real-life object and the digital twin. One method to adjust the adaptive gains is the use of the MIT rule. The principle of adaptation is developed at the Massachusetts Institute of Technology (hence the name MIT-rule) and aims to minimize the cost function given in Eqn. (13) due to the gains of K_x and K_r by analyzing the gradient of the indicator *Pi*. In our research, instead of calculating the differential of the variable $e(t)$ (see Eqn. 14), we adopted the increment of the variable (see Eqn. 15), and the results are presented in part 3.2 of Section 3.

Acknowledgements

Project co-financed by the European Regional Development Fund under the programme European Funds for Opolskie 2021–2027.

References

1. Bosikov I.I., Martyushev N.V., Klyuev R.V., Savchenko I.A., Kukartsev V.V., Kukartsev V.A., Tynchenko Y.A., *Modeling and complex analysis of the topology parameters of ventilation networks when ensuring fire safety while developing coal and gas deposits*, "Fire", Vol. 6, No. 3, DOI: 10.3390/fire6030095.
2. El-Afifi M.I., Team S., Elkelany M.M., *Development of fire detection technologies*, "Nile Journal of Communication and Computer Science", Vol. 7, No. 1, 2024, 58–66, DOI: 10.21608/njccs.2024.263103.1027.
3. Wang H., Fang X., Li Y., Zheng Z., Shen J., *Research and application of the underground fire detection technology based on multi-dimensional data fusion*, "Tunnelling and Underground Space Technology", Vol. 109, 2021, DOI: 10.1016/j.tust.2020.103753.
4. Huang L., Liu G., Wang Y., Yuan H., Chen T., *Fire detection in video surveillances using convolutional neural networks and wavelet transform*, "Engineering Applications of Artificial Intelligence", Vol. 110, 2022, DOI: 10.1016/j.engappai.2022.104737.
5. Mahaveerakannan R., Anitha C., Thomas A.K., Rajan S., Muthukumar T., Rajulu G.G., *An IoT based forest fire detection system using integration of cat swarm with LSTM model*, "Computer Communications", Vol. 211, 2023, 37–45, DOI: 10.1016/j.comcom.2023.08.020.
6. Dziarski K., Hulewicz A., *Uncertainty of thermographic temperature measurement of electric units contained in switchgear*, "Pomiary Automatyka Robotyka", Vol. 25, No. 4, 2021, 31–36, DOI: 10.14313/PAR_242/31.
7. Khan F., Xu Z., Sun J., Khan F.M., Ahmed A., Zhao Y., *Recent advances in sensors for fire detection*, "Sensors", Vol. 22, No. 9, 2022, DOI: 10.3390/s22093310.
8. James R.B., *New era in fire protection: The rise of Autonomous Robotic Fire Suppression (ARFS) Systems*, "International Fire Protection", No. 100, 2024, 90–94, [www.ifpmag.com].
9. Chen T., Yuan H., Su G., Fan W., *An automatic fire searching and suppression system for large spaces*, "Fire Safety Journal", Vol. 39, No. 4, 2004, 297–307, DOI: 10.1016/j.firesaf.2003.11.007.
10. Yuvaraj R, Senthil Kumar D., Bhalerao S.A., Murugesan K., Vellaiyan S., Van Minh N., *Real-time fire detection and suppression system using YOLO11n and Raspberry Pi for thermal safety applications*, "Case Studies in Thermal Engineering", Vol. 75, 2025, DOI: 10.1016/j.csite.2025.107159.
11. Talaat F.M., ZainEldin H., *An improved fire detection approach based on YOLO-v8 for smart cities*, "Neural computing and applications", Vol. 35, No. 28, 2023, 20 939–20 954, DOI: 10.1007/s00521-023-08809-1.
12. He Y., Hu J., Zeng M., Qian Y., Zhang R., *DCGC-YOLO: the efficient dual-channel bottleneck structure YOLO detection algorithm for fire detection*, "IEEE Access", Vol. 12, 2024, 65 254–65 265, DOI: 10.1109/ACCESS.2024.3385856.
13. McNeil J.G., Lattimer B.Y., *Robotic fire suppression through autonomous feedback control*, "Fire Technology", Vol. 53, No. 3, 22017, 1171–1199, DOI: 10.1007/s10694-016-0623-1.
14. Kustu T., Taskin A., *Deep learning and stereo vision based detection of post-earthquake fire geolocation for smart cities within the scope of disaster management: İstanbul case*, "International Journal of Disaster Risk Reduction", Vol. 96, 2023, DOI: 10.1016/j.ijdrr.2023.103906.
15. Latif A., Chung H., *Fire detection and spatial localization approach for autonomous suppression systems based on artificial intelligence*, "Fire Technology", Vol. 59, No. 5, 2023, 2621–2644, DOI: 10.1007/s10694-023-01426-3.
16. Gogoi D., Buragohain M., *Simulation of adaptive controller design with MRAC based on modified MIT rule*, "NeuroQuantology", Vol. 20, No. 10, 2022, 6663–6669, DOI: 10.14704/nq.2022.20.10.NQ55659.

Autonomiczny system działka gaśniczego – badania wstępne

Streszczenie: W artykule przedstawiono badania wstępne w celu opracowania algorytmu sterowania autonomicznym działkiem gaśniczym. Stosując metodę Lagrange'a wyznaczono model dynamiczny układu oraz przetestowano dwa algorytmy regulacji. Jak się okazało zastosowane sterowanie adaptacyjne, nawet przy parametrach obiektu różniących się od modelu o 10%, pozwoliło uzyskać zadawalające rezultaty regulacji. W pracy opisano także warstwę sprzętową opracowanego autorskiego prototypu, który składa się z działka gaśniczego, układu sterowania opartego na sterowniku programowalnym oraz z systemu wizyjnego pozwalającego na automatyczne lokalizowanie punktów wysokotemperaturowych w przestrzeni 3D.

Słowa kluczowe: działko gaśnicze, równania dynamiczne, sterowanie adaptacyjne, kinematyka odwrotna

Mateusz Pluskota, MSc Eng.
m.pluskota@kba-automatic.pl
ORCID: 0009-0008-9774-9312

He is a coordinator of the PLC Department at KBA AUTOMATIC and a graduate of the Opole University of Technology in Automation and Robotics, as well as Computer Science. An engineer specializing in the automation of industrial processes. He leads a team responsible for developing and implementing advanced solutions for control systems and drive synchronization in the logistics and manufacturing industries. He gained his experience through numerous implementation projects across Europe, where he managed project teams and conducted training sessions on new technologies and programming tools. He is actively involved in research and development activities, focusing on industrial system automation and the creation of innovative control algorithms.

Krzysztof Schwierz, MSc Eng.
k.schwierz@kba-automatic.pl
ORCID: 0009-0001-8246-4540

He is the coordinator of the R&D department and an automation systems engineer at KBA AUTOMATIC in Opole. A graduate of Automation and Robotics as well as Computer Science at the Opole University of Technology. He specializes in the design, simulation, and integration of advanced industrial automation systems, particularly in the logistics and manufacturing sectors. In his work, he combines engineering expertise with hands-on experience gained through both commercial and research--development projects. At KBA Automatic, he is responsible for coordinating project teams and implementing modern control and monitoring methods using PLC controllers, vision systems, and simulation tools.

Andrzej Neumann, Eng.
endrjuneu@gmail.com
ORCID: 0009-0009-1814-5738

He is a Master's student and a graduate engineer in Automation and Robotics, actively involved in several student research clubs focused on robotics and intelligent systems. He works in the R&D department as a Control Systems intern in a local company, where he gains experience in advanced automation solutions. His primary areas of interest include embedded systems, robotics, and modern control methods, with a particular focus on the application of neural networks in autonomous and mechatronic systems.

Dominik Fila, Eng.
dominikfila01@gmail.com
ORCID: 0009-0001-9554-1840

He is a master's student and a graduate engineer in automation and robotics. He is active in student clubs. Additionally, he works in the R&D department as an intern programmer, utilizing Python and C. His field of interest is embedded systems and industrial automation.

Łukasz Paczkowski, Eng.
lukaszpaczkowski@outlook.com
ORCID: 0009-0006-7270-2214

He received a Bachelor of Engineering degree in Automation and Robotics from the Opole University of Technology. He has been an active member of the Faculty Student Council and the president of the "PLC Team" Automation Student Research Group at Opole University of Technology. He conducts research on the use of active noise reduction in confined spaces. His engineering thesis focuses on a tracking algorithm utilizing neural networks for object detection to control a drone, and his interests span the broadest range of engineering, from automation systems to design.

Paweł Majewski, PhD Eng.
p.majewski@po.edu.pl
ORCID: 0000-0002-2344-8612

He received the B.Sc. degree, the M.Sc. degree in electrical engineering, and the Ph.D. degree in control engineering from the Opole University of Technology, Opole, Poland. From 2011 to 2016, he worked as a Constructor/Robot Programmer with Pawos Robotics Company. Since 2015, he has been employed with the Opole University of Technology. His research interests focus on the theoretical/practical development, of control algorithms in multivariable systems.